

Electronic Supplementary Information

**Long-lived emission beyond 1000 nm: Control of excited-state dynamics
in a dinuclear Tb(III)–Nd(III) complex**

Yuichi Kitagawa,^{*a,c} Kenji Matsuda,^b P. P. Ferreira da Rosa,^b Koji Fushimi,^a and
Yasuchika Hasegawa^{*a,c}

a. Faculty of Engineering, Hokkaido University, Kita-13, Nishi-8, Sapporo, Hokkaido,
060-8628, Japan.

b. Graduate School of Chemical Sciences and Engineering Hokkaido University, Kita-13,
Nishi-8, Sapporo, Hokkaido, 060-8628, Japan.

c. Institute for Chemical Reaction Design and Discovery (WPI-ICReDD), Hokkaido
University, Kita-21, Nishi-10, Sapporo, Hokkaido 001-0021, Japan.

Corresponding authors

E-mail: y-kitagawa@eng.hokudai.ac.jp (Yuichi Kitagawa);

hasegaway@eng.hokudai.ac.jp (Yasuchika Hasegawa)

Experimental section

General method: ^1H -NMR spectra were recorded in CD_2Cl_2 and CDCl_3 on a JEOL ECS-400 (400 MHz) spectrometer; TMS ($\delta_{\text{H}} = 0$ ppm) was used as the internal reference. Electrospray ionization (ESI) mass spectrometry was performed using JEOL JMS-T100 LP instrument. Elemental analyses were performed using MICRO CORDER JM10. Emission spectra and emission lifetimes were measured using a Horiba Fluorolog^{®3} spectrofluorometer under degassed condition. Emission quantum yields were measured using a FP-6300 spectrofluorometer with an integration sphere (ILF-533). Infrared spectra were measured using a JASCO FT/IR-4600 spectrometer. XRD data were recorded at on a Rigaku SmartLab diffractometer with $\text{Cu-K}\alpha$ radiation and D/teX Ultra detector.

Materials: Terbium chloride hexahydrate (99.9 %), ytterbium chloride hexahydrate (99.9 %), neodymium chloride hexahydrate (99.9 %), n-BuLi (in hexane, 1.6 M), magnesium sulfate, anhydrous (>98.0% (titration)), dichloromethane-d₂ (99.5%), and chloroform-d₁ (99.8%) were purchased from Kanto Chemical Co., Inc. Hydrogen peroxide (30 %) was purchased from Wako Pure Chemical Industries, Ltd. 2,2,6,6-Tetramethyl-3,5-heptanedione (> 97%), 1-bromo-4-iodobenzene (>98.0%), chlorodiphenylphosphine (> 98 %), and dichlorophenylphosphine (>98.0%) were purchased from Tokyo Chemical Industry Co., Ltd..

Preparation of dpb (1,4-bis(diphenylphosphoryl)benzene): We prepared the dpb ligand according to a previous report.^{S1}

IR (ATR): 1191 (st, P=O) cm⁻¹; Elemental analysis calcd. for C₃₀H₂₄O₂P₂: C, 75.31; H, 5.06%. Found: C, 74.86; H, 5.11%

Preparation of (4-bromophenyl)diphenylphosphine: A solution of n-BuLi (1.6 M in hexane, 19 ml, 31 mmol) was added dropwise to a solution of 1-bromo-4-iodobenzene (8.5 g, 30 mmol) in dry THF (80 mL) at -78 °C under Ar. After cooling for 45 min,

chlorodiphenylphosphine (5.5 mL, 30 mmol) was added to the solution, and then stirred for 17 h at room temperature. The product was evaporated, and extracted using dichloromethane, and the extract was washed with distilled water and then dried over anhydrous MgSO₄. The compounds were separated by silica gel chromatography (Hexane : CH₂Cl₂ = 3 : 1)

Yield: 76 % (6.99 g). ¹H-NMR (400 MHz, CD₂Cl₂): δ / ppm = 7.46-7.44 (m, 2H), 7.24-7.34 (m, 10H), 7.12-7.15 (m, 2H).

Preparation of dpppo (bis[p-(diphenylphosphoryl)phenyl]phosphine oxide): A solution of n-BuLi (1.6 M in hexane, 6.8 ml, 11 mmol) was added dropwise to a solution of (4-bromophenyl)diphenylphosphine (3.4 g, 10 mmol) in dry THF (50 mL) at -78 °C under Ar. After cooling for 30 minutes, dichlorophenylphosphine (0.7 mL, 5.5 mmol) was added to the solution, and then stirred for 3 h at room temperature. The product was evaporated, and extracted using dichloromethane, and the extract was washed with distilled water and then dried over anhydrous MgSO₄. The solution was cooled, and then 30% H₂O₂ aqueous solution (10 mL) was added. The reaction mixture was stirred for 4 h. The product was extracted using dichloromethane, and the extract was washed with distilled water and then dried over anhydrous MgSO₄. The compounds were separated by

silica gel chromatography (Ethyl acetate : methanol = 5 : 1)

Yield: 53 % (3.60 g). ^1H NMR (400 MHz, CDCl_3): δ (ppm) 7.70–7.81 (m, 8H), 7.61–7.70 (m, 10H), 7.54–7.60 (m, 5H), 7.44–7.53 (m, 10H); Elemental analysis calcd. for $\text{C}_{42}\text{H}_{33}\text{O}_3\text{P}_3$: C, 74.33 %; H, 4.90 %, found: C, 73.80 %; H, 4.82 %; ESI-MS (m/z): calcd. for $\text{C}_{42}\text{H}_{33}\text{NaO}_3\text{P}_3$ $[\text{M}+\text{Na}]^+$: 701.15, found: 701.15.

Preparation of $[\text{Tb}_2(\text{tmh})_6(\text{dpb})]$: A methanol solution (5 ml) containing dpb (55.9 mg, 0.12 mmol) was added to a methanol solution (5 ml) containing $[\text{Tb}_2(\text{tmh})_6]$ (170.1 mg, 0.12 mmol)^{S2}, and the mixed solution was refluxed for 5 h. The reactant solution was evaporated. The solid was dissolved into ethyl acetate and recrystallized. The obtained crystal was filtrated and washed with hexane to afford a colorless solid.

Yield: 57 % (108.8 mg). IR (ATR): 1573 (st, C=O), 1180 (st, P=O) cm^{-1} ; Elemental analysis calcd. for $\text{C}_{96}\text{H}_{138}\text{O}_{14}\text{P}_2\text{Tb}_2$: C, 60.82 %; H, 7.34 %, found: C, 60.49 %; H, 7.29 %; ESI-MS (m/z): calcd. for $\text{C}_{52}\text{H}_{62}\text{O}_6\text{P}_2\text{Tb}$ $[\text{Tb}(\text{tmh})_2(\text{dpb})]^+$: 1003.33, found: 1003.34.

Preparation of [Nd₂(tmh)₆(dpb)]: A methanol solution (5 ml) containing dpb (47.8 mg, 0.10 mmol) was added to a methanol solution (5 ml) containing [Nd₂(tmh)₆] (138.8 mg, 0.10 mmol)^{S2}, and the mixed solution was refluxed for 5 h. The reactant solution was evaporated. The solid was dissolved into ethyl acetate and recrystallized. The obtained crystal was filtrated and washed with hexane to afford a solid.

Yield: 49 % (91.2 mg). IR (ATR): 1573 (st, C=O), 1186 (st, P=O) cm⁻¹; Elemental analysis calcd. for C₁₀₀H₁₄₆Nd₂O₁₆P₂ [M+CH₃COOC₂H₅]: C, 61.45 %; H, 7.53 %, found: C, 60.59 %; H, 6.59 %

Preparation of [TbNd(tmh)₆(dpb)]: A methanol solution (5 ml) containing dpb (0.0478 m, 0.10 mmol) was added to a methanol solution (5 ml) containing [Nd₂(tmh)₆] (69.4 mg, 0.05 mmol) and [Tb₂(tmh)₆] (70.9 mg, 0.05 mmol), and the mixed solution was refluxed for 5 h. The reactant solution was evaporated. The solid was dissolved into ethyl acetate and recrystallized. The obtained crystal was filtrated and washed with hexane to afford a colorless solid.

Yield: 35 % (65.3 mg). IR (ATR): 1573 (st, C=O), 1181 (st, P=O) cm⁻¹; Elemental analysis calcd. for C₁₀₀H₁₄₆NdO₁₆P₂Tb [M+CH₃COOC₂H₅]: C, 60.99%; H, 7.47%, found: C, 60.03%; H, 7.20%.

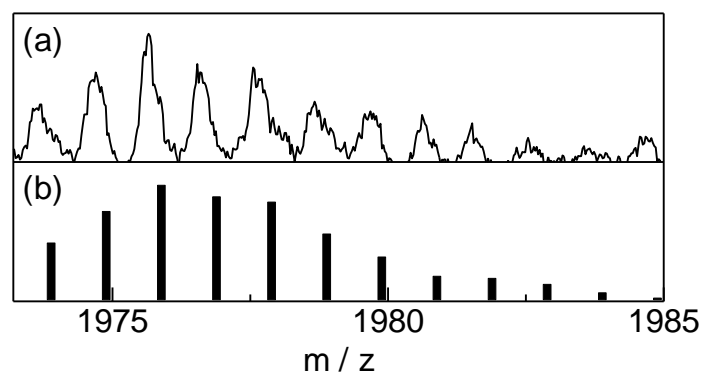


Fig. S1. Experimental ($[\text{TbNd}(\text{tmh})_6(\text{dpb})]$) and calculated mass spectra ($[\text{TbNd}(\text{tmh})_6(\text{dpb})+3\text{CH}_3\text{OH}]^+$). The ESI-MS measurements showed the existence of a $[\text{TbNd}(\text{tmh})_6(\text{dpb})]$ framework.

Preparation of $[\text{Tb}_3(\text{tmh})_9(\text{dpppo})]$: A methanol solution (5 ml) containing dpppo (0.0679 g, 0.10 mmol) was added to a methanol solution (5 ml) containing $[\text{Tb}_2(\text{tmh})_6]$ (0.2835 g, 0.20 mmol), and the mixed solution was refluxed for 5 h. The reactant solution was evaporated. The solid was dissolved into ethyl acetate and recrystallized. The obtained crystal was filtrated and washed with hexane to afford a colorless solid.

Yield: 67 % (186.9 mg). IR (ATR): 1572 (st, C=O), 1181 (st, P=O) cm^{-1} ; Elemental analysis calcd. for $\text{C}_{141}\text{H}_{204}\text{O}_{21}\text{P}_3\text{Tb}_3$: C, 60.38 %; H, 7.33 %, found: C, 59.87 %; H, 7.34 %. ESI-MS (m/z): calcd. for $\text{C}_{64}\text{H}_{71}\text{O}_7\text{P}_3\text{Tb}$ $[\text{Tb}(\text{tmh})_2\text{dpppo}]^+$: 1203.37, found: 1203.37.

Preparation of $[\text{Tb}_2\text{Nd}(\text{tmh})_9(\text{dpppo})]$: A methanol solution (5 ml) containing dpppo (0.0679 g, 0.10 mmol) was added to a methanol solution (5 ml) containing $[\text{Nd}_2(\text{tmh})_6]$ (0.0930 g, 0.067 mmol) and $[\text{Tb}_2(\text{tmh})_6]$ (0.1890 mg, 0.13 mmol), and the mixed solution was refluxed for 5 h. The reactant solution was evaporated. The solid was dissolved into ethyl acetate and recrystallized. The obtained crystal was filtrated and washed with hexane to afford a solid powder.

Yield: 35 % (98.2 mg). IR (ATR): 1572 (st, C=O), 1180 (st, P=O) cm^{-1} ; Elemental analysis calcd. for $\text{C}_{181}\text{H}_{284}\text{NdO}_{41}\text{P}_3\text{Tb}_2$ $[\text{M}+10\text{CH}_3\text{COOC}_2\text{H}_5]$: C, 59.22 %; H, 7.80 %, found: C, 58.22 %; H, 7.23 %.

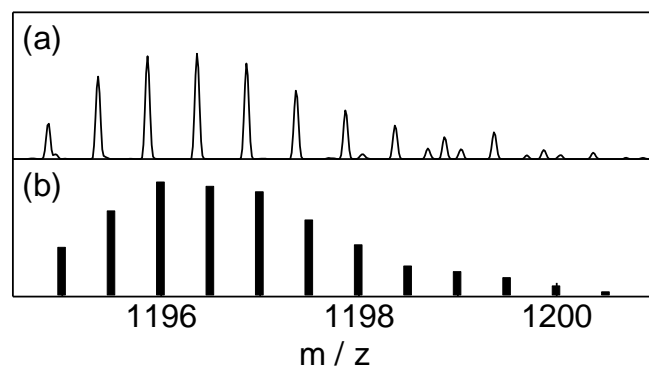


Fig. S2. Experimental ($[\text{Tb}_2\text{Nd}(\text{tmh})_6(\text{dpppo})]$) and calculated mass spectra ($[\text{TbNd}(\text{tmh})_6(\text{dpppo})+5\text{CH}_3\text{OH}+\text{CH}_3\text{COOC}_2\text{H}_5+2\text{Na}]^{2+}$). The ESI-MS measurements might show the existence of a $[\text{TbNd}(\text{tmh})_6(\text{dpppo})]$ framework.

Preparation of [Nd₃(tmh)₉dpppo]: A methanol solution (5 ml) containing dpppo (0.0679 g, 0.10 mmol) was added to a methanol solution (5 ml) containing [Nd₂(tmh)₆] (0.2776 g, 0.20 mmol), and the mixed solution was refluxed for 5 h. The solid was dissolved into ethyl acetate and recrystallized. The reactant solution was evaporated and washed with hexane to afford a solid powder.

Yield: 43 % (119.3 mg). IR (ATR): 1573 (st, C=O), 1186 (st, P=O) cm⁻¹; Elemental analysis calcd (%) for C₁₉₃H₃₀₈Nd₃O₄₇P₃ [M+13CH₃COOC₂H₅]; C 59.34, H 7.98, found: C 58.38, H 7.46.

Preparation of [Tb₂Yb(tmh)₉(dpppo)]: A methanol solution (5 ml) containing dpppo (0.0679 g, 0.10 mmol) was added to a methanol solution (5 ml) containing [Yb₂(tmh)₆] (0.0969 g, 0.067 mmol) and [Tb₂(tmh)₆] (0.1890 mg, 0.13 mmol), and the mixed solution was refluxed for 5 h. The reactant solution was evaporated. The solid was dissolved into ethyl acetate and recrystallized. The obtained crystal was filtrated and washed with hexane to afford a colorless solid.

Yield: 42 % (118.9 mg). IR (ATR): 1572 (st, C=O), 1182 (st, P=O) cm⁻¹; Elemental analysis calcd. for C₁₄₉H₂₂₀O₂₅P₃Tb₂Yb [M+2CH₃COOC₂H₅]: C, 59.75 %; H, 7.40 %, found: C, 58.80 %; H, 7.40 %.

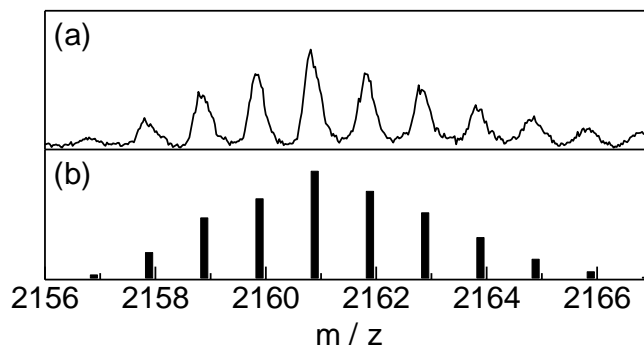


Fig. S3. Experimental ($[\text{Tb}_2\text{Yb}(\text{tmh})_9(\text{dpppo})]$) and calculated mass spectra ($[\text{TbYb}(\text{tmh})_6(\text{dpppo})+2\text{H}_2\text{O}]^+$). The ESI-MS measurements show the existence of a $[\text{TbYb}(\text{tmh})_6(\text{dpppo})]$ framework.

Preparation of $[\text{Yb}_3(\text{tmh})_9(\text{dpppo})]$: A methanol solution (5 ml) containing dpppo (0.0679 g, 0.10 mmol) was added to a methanol solution (5 ml) containing $[\text{Yb}_2(\text{tmh})_6]$ (0.2891 g, 0.20 mmol)^{S2}, and the mixed solution was refluxed for 5 h. The reactant solution was evaporated. The solid was dissolved into ethyl acetate and recrystallized. The obtained crystal was filtrated and washed with hexane to afford a colorless solid.

Yield: 67 % (186.9 mg). IR (ATR): 1574 (st, C=O), 1187 (st, P=O) cm^{-1} ; Elemental analysis calcd. for $\text{C}_{149}\text{H}_{220}\text{O}_{25}\text{P}_3\text{Yb}_3$ $[\text{M}+2\text{CH}_3\text{COOC}_2\text{H}_5]$: C, 59.19 %; H, 7.33 %, found: C, 58.46 %; H, 7.26 %. ESI-MS (m/z): calcd. for $\text{C}_{64}\text{H}_{71}\text{O}_7\text{P}_3\text{Yb}[\text{Yb}(\text{tmh})_2\text{dpppo}]^+$: 1218.38, found: 1218.46.

Single-Crystal X-ray Structure Determination

X-ray crystal structures and crystallographic data for $[\text{Tb}_2(\text{tmh})_6(\text{dpb})]$ and $[\text{Tb}_3(\text{tmh})_9(\text{dpppo})]$ are shown in Fig. 2, Fig. S6, and Tab. S1. Single crystals of the compounds were mounted on micromesh (MiTeGen M3-L19–25L) using paraffin oil. Measurements were made by using a Rigaku RAXIS RAPID (for $[\text{Tb}_2(\text{tmh})_6(\text{dpb})]$) imaging-plate area detector with graphite-monochromated Mo–K α radiation or a Rigaku VariMax RAPID (for $[\text{Tb}_3(\text{tmh})_9(\text{dpppo})]$) imaging-plate diffractometer with confocal mirror-monochromated Mo–K α radiation. All calculations were performed using a crystal-structure crystallographic software package. The CIF data were confirmed by the check CIF/PLATON service. These data (CCDC-1990682: $[\text{Tb}_2(\text{tmh})_6(\text{dpb})]$ and CCDC-1990683: $[\text{Tb}_3(\text{tmh})_9(\text{dpppo})]$) can be obtained free of charge from The Cambridge Crystallographic Data Centre via www.ccdc.cam.ac.uk/data_request/cif.

Tab. S1. Crystal data of [Tb₂(tmh)₆(dpb)] and [Tb₃(tmh)₉(dpppo)]

	[Tb ₂ (tmh) ₆ (dpb)]	[Tb ₃ (tmh) ₉ (dpppo)]
chemical formula	C ₉₈ H ₁₃₈ O ₁₄ P ₂ Tb ₂	C ₁₄₁ H ₂₀₄ O ₂₁ P ₃ Tb ₃
formula weight	1919.86	2804.70
crystal system	Triclinic	Orthorhombic
space group	P-1	P2 ₁ 2 ₁ 2 ₁
a / Å	13.4524 (5)	17.3827 (3)
b / Å	16.5651 (6)	22.9977 (4)
c / Å	22.9953 (9)	38.2920 (6)
α / deg	88.5491 (13)	90
β / deg	75.5823 (11)	90
γ / deg	87.8446 (11)	90
volume / Å ³	4958.7 (3)	15307.7 (4)
Z	2	4
density / g cm ⁻³	1.286	1.460
Temperature / °C	-150	-150
R	0.0700	0.0398
wR ₂	0.1693	0.0949

Tab. S2. Shape measure calculation results

	C _{2v}	C _{3v}
[Tb ₂ (tmh) ₆ (dpb)]	0.468	1.480
[Tb ₃ (tmh) ₉ (dpppo)] (Side Tb)	1.640	0.381
[Tb ₃ (tmh) ₉ (dpppo)] (Middle Tb)	0.468	1.480

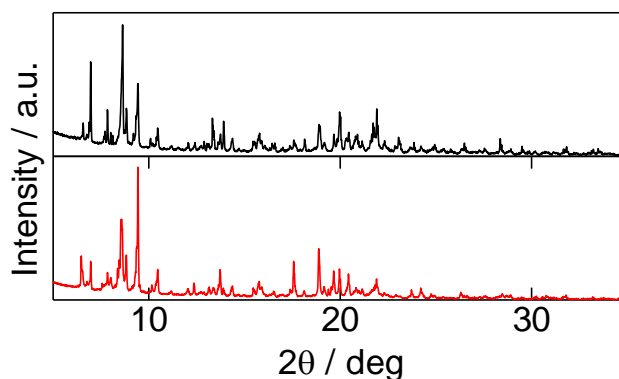


Fig. S4. XRD patterns of $[\text{Tb}_2(\text{tmh})_6(\text{dpb})]$ (black line) and $[\text{TbNd}(\text{tmh})_6(\text{dpb})]$ (red line).

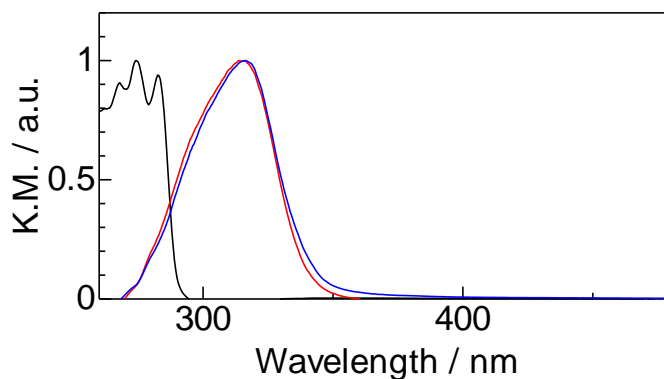


Fig. S5. Diffuse reflectance spectra of dpb ligand (black line), $[\text{Tb}_2(\text{tmh})_6(\text{dpb})]$ (red line), and $[\text{TbNd}(\text{tmh})_6(\text{dpb})]$ (blue line). The samples were 100-fold dilution using KBr. The spectra are normalized by intensity maxima. The diffuse reflectance spectra indicate that the selective excitation of tmh ligands is occurred for the measurement of emission spectra ($\lambda_{\text{ex}} = 330 \text{ nm}$), lifetimes ($\lambda_{\text{ex}} = 356 \text{ nm}$), and emission quantum yields ($\lambda_{\text{ex}} = 360 \text{ nm}$).

Comparative study for understanding photophysics using lanthanide-lanthanide energy transfer

We prepared trinuclear Ln(III)-Ln(III)-Ln(III) (Ln = Tb or Nd or Yb) complexes (Fig. S6a), a hetero-trinuclear Tb(III)-Tb(III)-Nd(III) complex, and a hetero-trinuclear Tb(III)-Tb(III)-Yb(III) complex for elucidating lanthanide-lanthanide energy transfer. In this study, dpppo (bis[p-(diphenylphosphoryl)phenyl]phosphine oxide) ligand was used as a nano-spacer. The single crystals of the trinuclear Tb(III)-Tb(III)-Tb(III) complex were obtained by recrystallization from an ethyl acetate solution. The crystal structure (Fig. S6b) was found to be orthorhombic, with space group $P2_12_12_1$ (for the crystallographic data, see Table S1, ESI†). The coordination site in the Tb(III) complex comprised three tmh ligands and one phosphine oxide ligand as a nano-spacer, such that the coordination geometries around the Tb(III) ions consisted of a characteristic 7-coordinated capped octahedron and a capped trigonal prism (Tab. S2).^{S3} The intra- and intermolecular distances between the Tb(III) ions were about 1.1 (1.3) and 1.2 nm, respectively. The heterotrinuclear Tb(III)-Tb(III)-Nd(III) and Tb(III)-Tb(III)-Yb(III) complexes were prepared by the complexation of $[Tb_2(tmh)_6]$ and $[Ln_2(tmh)_6]$ (Ln = Nd or Yb) with dpppo in methanol. The XRD patterns of these heteronuclear complexes were similar to that of the trinuclear Tb(III)-Tb(III)-Tb(III) complex (Fig. S7).

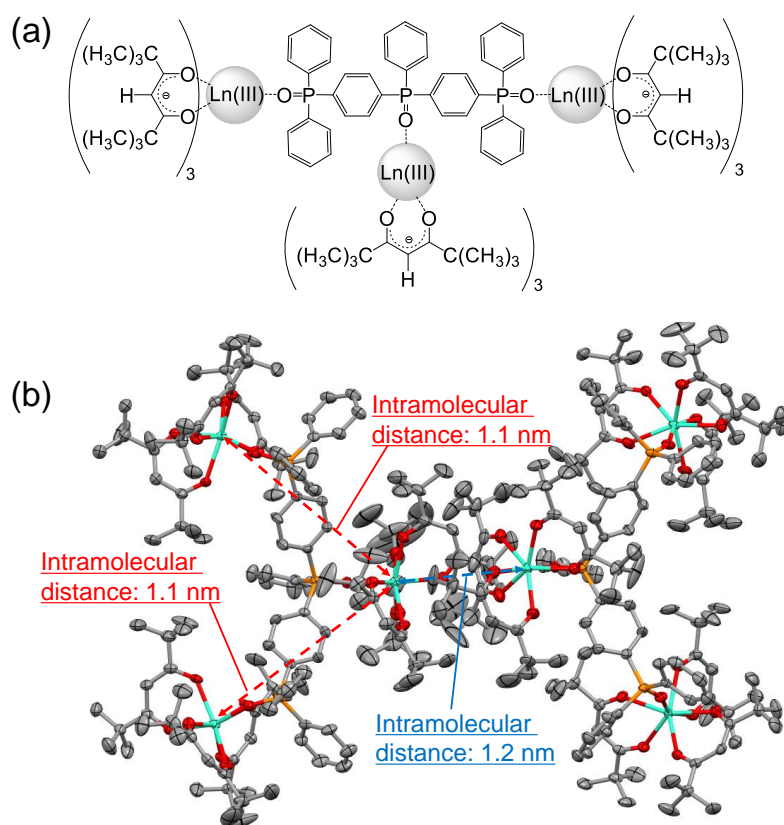


Fig. S6. (a) Chemical structure of a trinuclear Ln(III) complex. (b) ORTEP drawing (ellipsoid probability: 50%) of the trinuclear Tb(III) complex.

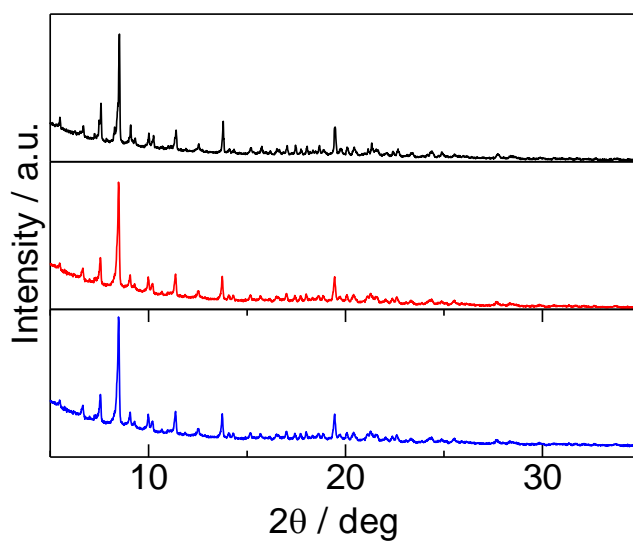


Fig. S7. XRD patterns of $[\text{Tb}_3(\text{tmh})_9(\text{dpppo})]$ (black line), $[\text{Tb}_2\text{Nd}(\text{tmh})_6(\text{dpppo})]$ (red line), and $[\text{Tb}_2\text{Yb}(\text{tmh})_6(\text{dpppo})]$ (blue line).

The emission spectra of $[\text{Tb}_3(\text{tmh})_9(\text{dpppo})]$, $[\text{Tb}_2\text{Nd}(\text{tmh})_9(\text{dpppo})]$, and $[\text{Nd}_3(\text{tmh})_9(\text{dpppo})]$ at RT are shown in Fig. S8. The emission peaks of $[\text{Tb}_3(\text{tmh})_9(\text{dpppo})]$ and $[\text{Tb}_2\text{Nd}(\text{tmh})_9(\text{dpppo})]$ at 491, 548, 583, 618, and 655 nm were assigned to the ${}^5\text{D}_4 \rightarrow {}^7\text{F}_6$, ${}^5\text{D}_4 \rightarrow {}^7\text{F}_5$, ${}^5\text{D}_4 \rightarrow {}^7\text{F}_4$, ${}^5\text{D}_4 \rightarrow {}^7\text{F}_3$, and ${}^5\text{D}_4 \rightarrow {}^7\text{F}_2$ transitions, respectively, of Tb(III) ions (Fig. S8). The similar shapes of the emission spectra of $[\text{Tb}_3(\text{tmh})_9(\text{dpppo})]$ and $[\text{Tb}_2\text{Nd}(\text{tmh})_9(\text{dpppo})]$ indicated the formation of similar coordination geometries around the Tb(III) ion. The emission peaks of $[\text{Nd}_3(\text{tmh})_9(\text{dpppo})]$ and $[\text{Tb}_2\text{Nd}(\text{tmh})_9(\text{dpppo})]$ at 877 and 1057 nm were assigned to the ${}^4\text{F}_{3/2} \rightarrow {}^4\text{I}_{9/2}$ and ${}^4\text{F}_{3/2} \rightarrow {}^4\text{I}_{11/2}$ transitions, respectively, of Nd(III) ions.

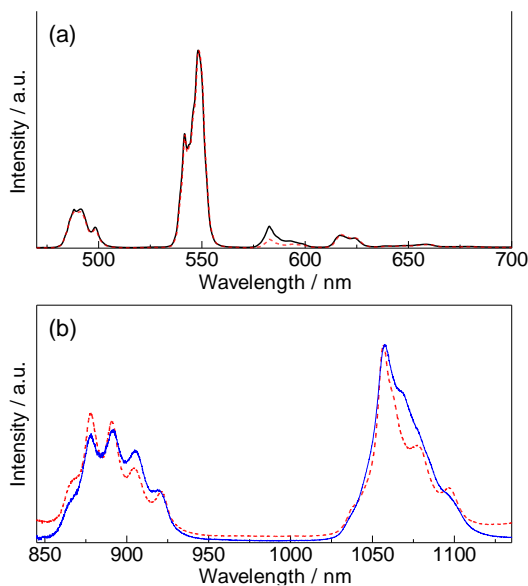


Fig. S8. Emission spectra of $[\text{Tb}_3(\text{tmh})_9(\text{dpppo})]$ (black line, $\lambda_{\text{ex}} = 330$ nm), $[\text{Tb}_2\text{Nd}(\text{tmh})_9(\text{dpppo})]$ (red broken line, $\lambda_{\text{ex}} = 330$ nm), and $[\text{Nd}_3(\text{tmh})_9(\text{dpppo})]$ (blue line, $\lambda_{\text{ex}} = 590$ nm). The spectra are normalized by intensity maxima: (a) detection of Tb(III) emission and (b) detection of Nd(III) emission.

We also investigated the emission lifetimes of $[\text{Tb}_3(\text{tmh})_9(\text{dpppo})]$, $[\text{Tb}_2\text{Nd}(\text{tmh})_9(\text{dpppo})]$, and $[\text{Nd}_3(\text{tmh})_9(\text{dpppo})]$ at RT, as summarized in Tab. S3. The time-resolved Nd(III) emission of $[\text{Tb}_2\text{Nd}(\text{tmh})_9(\text{dpppo})]$ showed a multiexponential decay (Fig. S9). The emission lifetimes were estimated to be 0.83, 99, and 280 μs . The shortest lifetime component ($\tau = 0.83 \mu\text{s}$) was consistent with the lifetime of $[\text{Nd}_3(\text{tmh})_9(\text{dpppo})]$ ($\tau = 0.90 \mu\text{s}$). The intermolecular distance (11.9 \AA) between lanthanide ions is longer than the intramolecular distance (10.6 \AA). At this stage, we consider that the 99- μs and 280- μs emission lifetime components were associated with the intra- and inter-molecular energy transfer, respectively. In this study, we compared the emission lifetimes of the trinuclear complex (99 μs and 280 μs) with that of the dinuclear complex. The nearest intramolecular distance between lanthanide ions in the trinuclear complex (10.6 \AA) is longer than that in the dinuclear complex (10.0 \AA), leading to longer emission lifetime for the trinuclear complex (99 $\mu\text{s} > 78 \mu\text{s}$). The nearest intermolecular distance between lanthanide ions of trinuclear complex (11.6 \AA) is slightly shorter to that of dinuclear complex (11.9 \AA), which might lead to slightly shorter emission lifetime for the trinuclear complex (280 $\mu\text{s} < 290 \mu\text{s}$). These results suggest that the distance between lanthanide ions is critical for determining the rate of energy transfer from Tb(III) to Nd(III) ion. We also measured the Nd(III) and Tb(III) emission lifetimes in the ground

and mixed powder of $[\text{Nd}_3(\text{tmh})_9(\text{dpppo})]$ and $[\text{Tb}_3(\text{tmh})_9(\text{dpppo})]$ (Fig. S10). Effective emission lifetime changes were not observed, indicating that energy transfer occurred in a crystal state.

Tab. S3. Photophysical properties of trinuclear Ln(III) complexes in solid powder states at RT.

	$\tau_{\text{Tb}} / \mu\text{s}^{[a]}$	$\tau_{\text{Nd}} / \mu\text{s}^{[b]}$	$\tau_{\text{Yb}} / \mu\text{s}^{[b]}$	$\Phi_{\text{Tb}} / \%^{[c]}$
$[\text{Tb}_3(\text{tmh})_9(\text{dpppo})]$	720	-	-	69
$[\text{Tb}_2\text{Nd}(\text{tmh})_9(\text{dpppo})]$	170, 490	0.83, 99, 280	-	16
$[\text{Nd}_3(\text{tmh})_9(\text{dpppo})]$	-	0.90	-	-

[a] $\lambda_{\text{ex}} = 356 \text{ nm}$, $\lambda_{\text{em}} = 547 \text{ nm}$, [b] $\lambda_{\text{ex}} = 356 \text{ nm}$, $\lambda_{\text{em}} = 1057 \text{ nm}$, [c] $\lambda_{\text{ex}} = 360 \text{ nm}$.

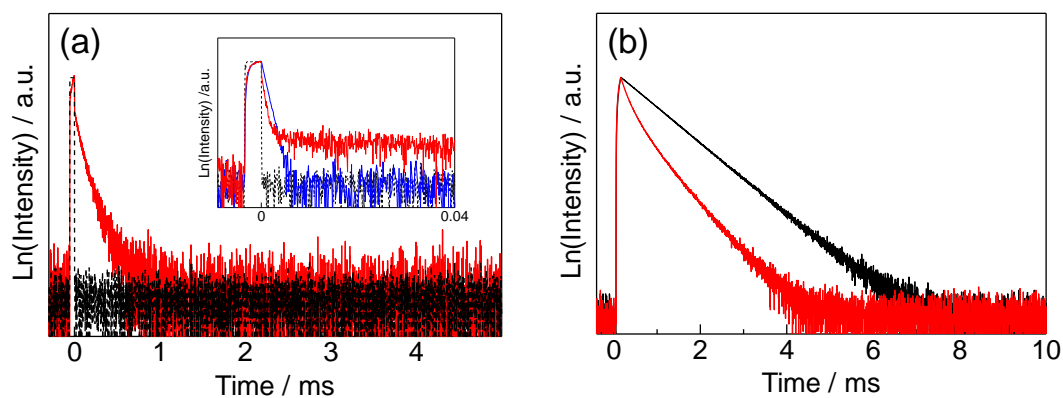


Fig. S9. (a) Time-resolved Nd(III) emission ($\lambda_{\text{em}} = 1057 \text{ nm}$) of $[\text{Tb}_2\text{Nd}(\text{tmh})_9(\text{dpppo})]$ (red line) and instrument response function (black line). Inset: Time-resolved Nd(III) emissions ($\lambda_{\text{em}} = 1057 \text{ nm}$) of $[\text{Tb}_2\text{Nd}(\text{tmh})_9(\text{dpppo})]$ (red line), $[\text{Nd}_3(\text{tmh})_9(\text{dpppo})]$ (blue line), and instrument response function (black line). (b) Time-resolved Tb(III) emissions ($\lambda_{\text{em}} = 548 \text{ nm}$) of $[\text{Tb}_3(\text{tmh})_9(\text{dpppo})]$ (black line) and $[\text{Tb}_2\text{Nd}(\text{tmh})_9(\text{dpppo})]$ (red line).

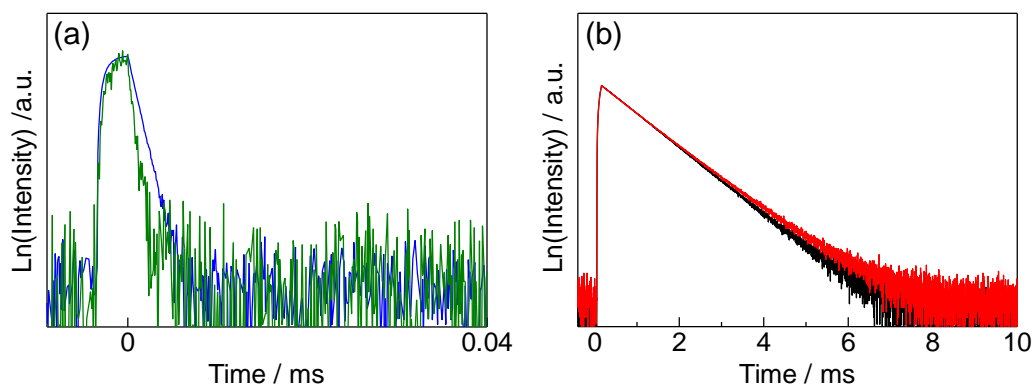


Fig. S10. (a) Time-resolved Nd(III) emissions ($\lambda_{em} = 1057$ nm) of $[\text{Nd}_3(\text{tmh})_9(\text{dpppo})]$ (blue line) and ground and mixed powder of $[\text{Nd}_3(\text{tmh})_9(\text{dpppo})]$ and $[\text{Tb}_3(\text{tmh})_9(\text{dpppo})]$ (green line). (b) Time-resolved Tb(III) emissions ($\lambda_{em} = 548$ nm) of $[\text{Tb}_3(\text{tmh})_9(\text{dpppo})]$ (black line) and ground and mixed powder of $[\text{Nd}_3(\text{tmh})_9(\text{dpppo})]$ and $[\text{Tb}_3(\text{tmh})_9(\text{dpppo})]$ (red line)

The emission spectra of $[\text{Tb}_3(\text{tmh})_9(\text{dpppo})]$, $[\text{Tb}_2\text{Yb}(\text{tmh})_9(\text{dpppo})]$, and $[\text{Yb}_3(\text{tmh})_9(\text{dpppo})]$ at RT are shown in Fig. S11. The emission peaks of $[\text{Tb}_3(\text{tmh})_9(\text{dpppo})]$ and $[\text{Tb}_2\text{Yb}(\text{tmh})_9(\text{dpppo})]$ at 491, 548, 583, 618, and 655 nm were assigned to the $^5\text{D}_4 \rightarrow ^7\text{F}_6$, $^5\text{D}_4 \rightarrow ^7\text{F}_5$, $^5\text{D}_4 \rightarrow ^7\text{F}_4$, $^5\text{D}_4 \rightarrow ^7\text{F}_3$, and $^5\text{D}_4 \rightarrow ^7\text{F}_2$ transitions, respectively, of Tb(III) ions (Fig. S11a). The similar shapes of the $[\text{Tb}_3(\text{tmh})_9(\text{dpppo})]$ and $[\text{Tb}_2\text{Yb}(\text{tmh})_9(\text{dpppo})]$ emission spectra indicated the formation of similar coordination geometries around the Tb(III) ion. The emission peaks of $[\text{Yb}_3(\text{tmh})_9(\text{dpppo})]$ and $[\text{Tb}_2\text{Yb}(\text{tmh})_9(\text{dpppo})]$ at 975 nm (Fig S11b) were assigned to the $^2\text{F}_{5/2} \rightarrow ^7\text{F}_{7/2}$ transition. No effective Yb and Tb emission decay change between $[\text{Tb}_2\text{Yb}(\text{tmh})_9(\text{dpppo})]$ and $[\text{Ln}_3(\text{tmh})_9(\text{dpppo})]$ ($\text{Ln} = \text{Tb}$

and Yb) was observed (Fig. S12), indicating that the energy transfer from Tb(III) ion to Yb(III) ion was ineffective. This was probably because the luminescent bands of Tb(III) ions (491, 548, 583, and 618 nm) are not close to the absorption bands of Yb(III) at ~970 nm.^{S4}

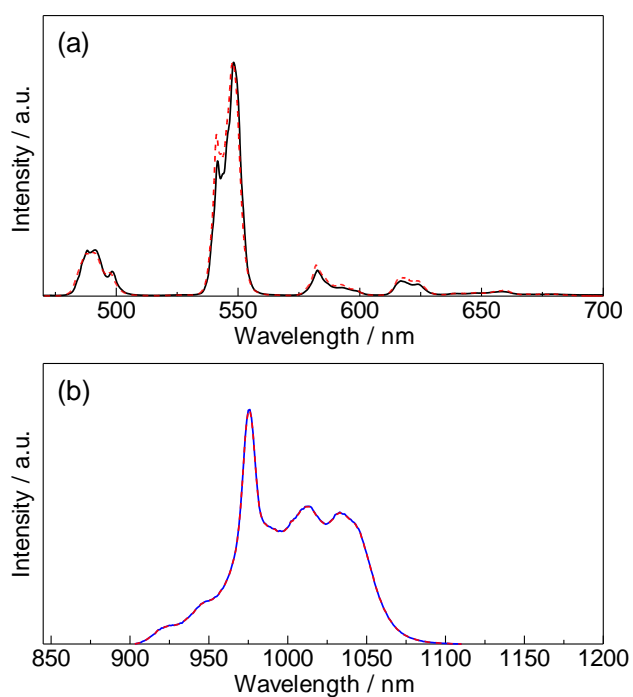


Fig. S11. (a) Emission spectra of [Tb₃(tmh)₉(dpppo)] (black line, $\lambda_{\text{ex}} = 330$ nm), [Tb₂Yb(tmh)₉(dpppo)] (red broken line, $\lambda_{\text{ex}} = 330$ nm), and [Yb₃(tmh)₉(dpppo)] (blue line, $\lambda_{\text{ex}} = 330$ nm): (a) detection of Tb(III) emission and (b) detection of Yb(III) emission.

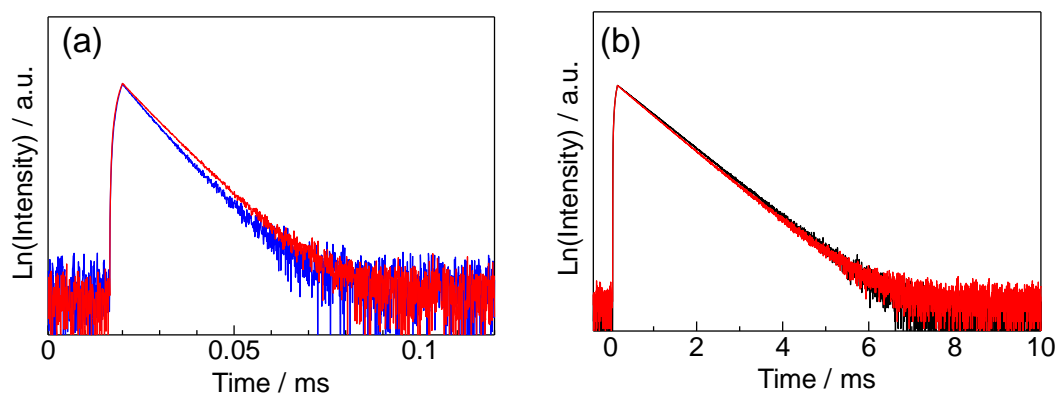


Fig. S12. (a) Time-resolved Yb(III) emissions ($\lambda_{\text{em}} = 1057$ nm) of $[\text{Tb}_2\text{Yb}(\text{tmh})_9(\text{dpppo})]$ (red line) and $[\text{Yb}_3(\text{tmh})_9(\text{dpppo})]$ (blue line). (b) Time-resolved Tb(III) emissions ($\lambda_{\text{em}} = 548$ nm) of $[\text{Tb}_3(\text{tmh})_9(\text{dpppo})]$ (black line) and $[\text{Tb}_2\text{Yb}(\text{tmh})_9(\text{dpppo})]$ (red line).

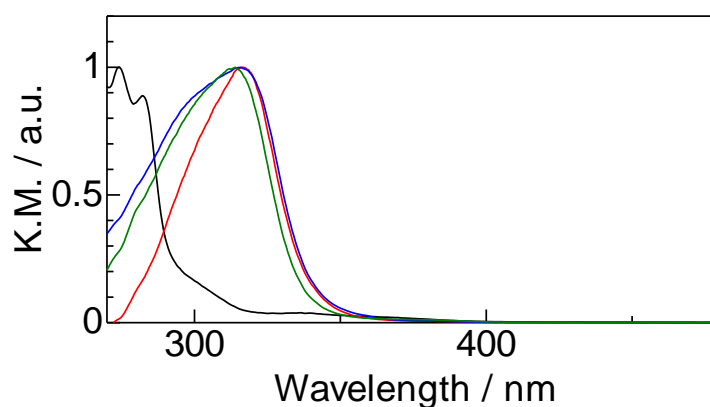


Fig. S13. Diffuse reflectance spectra of dpppo ligand (black line), $[\text{Tb}_3(\text{tmh})_9(\text{dpppo})]$ (red line), $[\text{Tb}_2\text{Nd}(\text{tmh})_9(\text{dpppo})]$ (blue line), and $[\text{Tb}_2\text{Yb}(\text{tmh})_6(\text{dpppo})]$ (green line). The samples used were diluted 100-fold using KBr. The spectra are normalized in terms of intensity maxima. These spectra indicate that the selective excitation of tmh ligands occurred for the measurement of emission spectra ($\lambda_{\text{ex}} = 330$ nm), lifetimes ($\lambda_{\text{ex}} = 356$ nm), and emission quantum yields ($\lambda_{\text{ex}} = 360$ nm).

Fitting parameter for emission decay analysis

We used Decay Analysis Software v6.8 for emission lifetime analysis.

One exponential: $A+B1*EXP(-i/T1)$

Two exponentials: $A+B1*EXP(-i/T1) +B2*EXP(-i/T2)$

1. [Tb₂(tmh)₆(dpb)]

1-1. Tb(III) emission

T1 = 300.7895 ch, 8.021069E-04 sec (S.Dev = 2.236448E-07 sec)

A = 30.77479 (S.Dev = 0.1785773)

B1 = 52804.12 [100.00 Rel.Ampl] (S.Dev = 13.33349)

2. [TbNd(tmh)₆(dpb)]

2-1. Tb(III) emission

T1 = 247.8876 ch, 6.610349E-04 sec (S.Dev = 1.01104E-06 sec)

T2 = 103.7506 ch, 2.766689E-04 sec (S.Dev = 7.75121E-07 sec)

A = 17.18693 (S.Dev = 0.1077733)

B1 = 22192.22 [68.65 Rel.Ampl] (S.Dev = 17.89954)

B2 = 24211.28 [31.35 Rel.Ampl] (S.Dev = 38.92216)

2-2. Nd(III) emission

Long components

T1 = 58.69808 ch, 7.826427E-05 sec (S.Dev = 2.365691E-06 sec)

T2 = 214.9916 ch, 2.866561E-04 sec (S.Dev = 3.482027E-06 sec)

A = 8899.725 (S.Dev = 4.143334)

B1 = 5384.509 [23.19 Rel.Ampl] (S.Dev = 41.76918)

B2 = 4868.896 [76.81 Rel.Ampl] (S.Dev = 23.91975)

Short components

T1 = 9.770375 ch, 8.141996E-07 sec (S.Dev = 5.129706E-09 sec)

A = 3507.605 (S.Dev = 4.774413)

B1 = 19881.89 [100.00 Rel.Ampl][1.00 Alpha] (S.Dev = 55.12317)

3. [Nd(tmh)₆(dpb)]

3-1. Nd(III) emission

T1 = 12.15142 ch, 1.012621E-06 sec (S.Dev = 1.613698E-08 sec)

A = 3205.281 (S.Dev = 4.996471)

B1 = 3261.202 [100.00 Rel.Ampl] (S.Dev = 30.47378)

4. [Tb₃(tmh)₆(dpppo)]

4-1. Tb(III) emission

T1 = 269.8959 ch, 7.197239E-04 sec (S.Dev = 2.666672E-20 sec)

A = 12.72742 (S.Dev = 9.637973E-02)

B1 = 53865.06 [100.00 Rel.Ampl] (S.Dev = 14.1507)

5. [Tb₂Nd(tmh)₆(dpppo)]

5-1. Tb(III) emission

T1 = 62.32287 ch, 1.661947E-04 sec (S.Dev = 7.78185E-07 sec)

T2 = 183.901 ch, 4.904037E-04 sec (S.Dev = 5.849576E-07 sec)

A = 14.80685 (S.Dev = 8.220839E-02)

B1 = 28825.91 [36.11 Rel.Ampl] (S.Dev = 43.10474)

B2 = 17281.41 [63.89 Rel.Ampl] (S.Dev = 16.10327)

5-2. Nd(III) emission

(Long components)

T1 = 212.5556 ch, 2.83408E-04 sec (S.Dev = 7.067118E-06 sec)

T2 = 74.0494 ch, 9.873274E-05 sec (S.Dev = 6.638168E-07 sec)

A = 11995.71 (S.Dev = 2.044296)

B1 = 4767.708 [50.03 Rel.Ampl] (S.Dev = 26.82746)

B2 = 13666.8 [49.97 Rel.Ampl] (S.Dev = 48.67609)

(Short component)

T1 = 10.01924 ch, 8.349383E-07 sec (S.Dev = 2.655181E-08 sec)

A = 2258.66 (S.Dev = 3.036299)

B1 = 1480.686 [100.00 Rel.Ampl][1.00 Alpha] (S.Dev = 25.08619)

6. [Nd₃(tmh)₆(dpppo)]

T1 = 10.76637 ch, 8.971996E-07 sec (S.Dev = 5.633157E-09 sec)

A = 7543.009 (S.Dev = 12.05993)

B1 = 23949.72 [100.00 Rel.Ampl] (S.Dev = 68.5882)

References

S1. M. Yamamoto, Y. Kitagawa, T. Nakanishi, K. Fushimi and Y. Hasegawa, *Chem. –*

Eur. J. **2018**, 24, 17719–17726.

S2. Fulgêncio, F. C. De Oliveira, F. F. Ivashita, A. Paesano, D. Windmüller, A. Marques-

Netto, W. F. Magalhães and J. C. MacHado, *Spectrochim. Acta, Part A* **2012**, 92,

415–418.

S3. D. Casanova, M. Llunell, P. Alemany and S. Alvarez, *Chem. – Eur. J.* **2005**, 11,

1479–1494.

S4. S. Kishimoto, T. Nakagawa, T. Kawai, Y. Hasegawa, *Bull. Chem. Soc. Jpn.* **2011**,

84, 148.